A&A 393, 1081–1087 (2002)
DOI: 10.1051/0004-6361:20021101

Astronomy & Astrophysics

L-photoionization of atomic aluminium: production of Al II, Al III and Al IV UV lines

A. G. Kochur[1], D. Petrini[2], and E. P. da Silva[3]

[1] Rostov State University of Transport Communication, 344038 Rostov–on–Don, Russia
e-mail: agk@jeo.ru
[2] Observatoire de la Côte d'Azur, CNRS Laboratoire Cassini, BP 4229, 06304 Nice Cedex 4, France
[3] Departamento de Física, U.F.C., CP 6030, Fortaleza 60455–760, Ceará, Brazil
e-mail: euclimar@fisica.ufc.br

Received 26 March 2002 / Accepted 3 July 2002

Abstract. Aluminium atoms undergoing soft X–ray irradiation produce multiply–ionized ions in excited states through inner–shell photoionization followed by radiationless transitions, i.e. Auger cascades. Photoionization of 2s–, 2p– and 3s subshells are considered for the 80 eV to 1 keV incident photon energy range. Photoionization cross sections, shake probabilities and Auger and Coster–Kronig rates are evaluated in various approximations. Al II, Al III and Al IV UV lines are directly produced independently of local temperature and electron density. Monopole shake up/off and conjugate shake up excitations are important over a large energy interval beyond the L thresholds.

Key words. atomic data – atomic processes – line: formation

1. Introduction

Ionization potentials for 2s and 2p subshells of the third row elements range respectively from 75.161 and 21.581 eV for atomic sodium up to 281.80 and 250.21 eV for argon (Indelicato et al. 1998). In some peculiar astrophysical situations, such as planetary nebula haloes or in the vicinity of soft X–ray sources, where densities and temperatures are low, a few hundred eV photons are often present and give rise, through photoionization and consecutive Auger cascades, to multiply ionized atoms. Other cases are early–type stars producing shock X–rays transferred by stellar wind, and stellar sources located near normal galaxies surrounded by a local interstellar medium. Generally the ionized atoms are excited and consequently distinct groups of UV lines are emitted.

The consequences of inner–shell photoionization followed by Auger decays has been often considered in the equations of balance of successive ionization stages for optically thin plasma in the vicinity of a point source of X–rays. For example Weisheit (1974) treated the case of silicon in an interstellar medium undergoing soft–X–ray irradiation. Most of the silicon is of course Si II, however, Si III, Si IV and Si V are also strongly affected. The interest in those studies was focused on the double ionization of the target; single inner–shell photoionization followed by radiationless decay was considered. No attention was however payed to the details of the ionization process, such as shake and double shake processes, Auger shake processes, and direct production of lines issued from successive ionization stages.

In our previous work (Kochur et al. 2001) we addressed the case of the L–shell photoionization of atomic Mg. While 2p–ionization leads to the Mg III ground term, for 2s–ionization the production of the Mg III $2p^5 3s\ {}^1P^o$ term is favored, giving rise to the 231.73 Å line.

We now proceed to the case of Al where the presence of 3s and 3p electrons makes the decay processes more complex. We consider line emission during the cascading decays of the following 2s– and 2p–hole states:

1. Single inner–shell vacancy states produced by single photoionization, here $2s2p^6 3s^2 3p$ and $2s^2 2p^5 3s^2 3p$.
2. The states with one outer electron ($n = 3$) either shaken up (SU) or shaken off (SO) through a monopole mechanism (Carlson & Nestor 1973). Monopole processes are those additional excitations/ionizations that occur without change of the orbital angular momentum quantum number. Here, for example, upon 2s–ionization: $2s2p^6 3s^2$ and 3s3p (SO), $2s2p^6 3s^2 4p$ and 3s3p4s (SU). We also consider the states produced by double monopole shake processes (dS), when two outermost–shell electrons are either shaken up or off simultaneously.
3. The states produced through dipole excitations i.e. *conjugate* shake up (cSU) processes (Badnell et al. 1997). Of these, the strongest are the cSU without change of the principal quantum number n, i.e. 3p→3d and 3s→3p excitations which, for example for 2p–photoionization, lead to

Send offprint requests to: D. Petrini, e-mail: petrini@obs-nice.fr

formation of the states $2p^5 3s 3p^2$ and $2p^5 3s^2 3d$. The cSU processes may be understood as being due to the collisional effect induced by an outgoing photoelectron.

In the following discussion, shake process probabilities upon 2s– or 2p–ionization are given as ratios to respective single process probabilities. Photon energies, both for 2s and 2p vacancy creation, are given in dimensionless units of X, defined as the ratio of the incident photon energy to the 2s ionization potential.

For compactness, we shall identify, for example, the SU 3p→4p upon 2s ionization by the notation 2s/SU 3p→4p. In the same manner, we shall abbreviate the conjugate shake up processes, for example, 2p/cSU3p→3d. Double shake processes are referred to as, for example, 2s/dS 3s3p→ $\{n', \varepsilon'\}$s, $\{n'', \varepsilon''\}$p.

The $1s^2$ is not mentioned hereafter when identifying configurations.

2. Theory

2.1. Photoionization cross sections

We calculate 2s and 2p photoionization cross sections both in the one–configuration approximation and using the R-matrix technique based on the close coupling theory (Berrington et al. 1995).

In the one–configuration scheme, we used the Pauli–Fock core and continuous spectrum wavefunctions obtained by averaging the electrostatic interaction over the configuration (Kau et al. 1997). The calculations are performed in the relaxed-core approximation accounting for the rearrangement of atomic residue upon creation of an inner-shell vacancy (Amusia & Cherepkov 1975; Sukhorukov et al. 1979)

In the R–matrix approach, which concerns only single, SU and cSU cross sections, configuration interaction (CI) is present both in the description of the initial and residual term wavefunctions. Free channel coupling is fully taken into account as well as exchange potentials (a priori not negligible for low free l quantum number). Dipole channel coupling is responsible for the cSU effects. The *closed channel* system $Al^+ + e^-\ {}^2P^o$ defines the Al ground state wavefunction, and 3 even allowed symmetries S, P, D, for the free final wave functions are necessary for obtaining the residual term cross sections.

Although in such a model the same set of basic orbitals is used for both ground and 2s/2p vacancy states, the inclusion of CI between, for example, $2s2p^6 3s^2 3p$ and 4p improves the 2s vacancy state description. In a more thorough but tedious calculation, additional pseudo–orbitals could be introduced to obtain improved CI wavefunctions for the residual ion.

The cross sections are calculated with length formulae.

In the case of 2s–photoionization, to describe the free systems $Al^+ + e^-$, the products of soft X–ray photoionization leading to single, SU and cSU processes, we chose two sets of Al^+ residual configurations. Ground configurations: $2s^2 2p^6 3s^2$, 3s3p, $3p^2$, 3s4s, 3s4p, 3s3d, and 2s–hole configurations: $2s2p^6 3s^2 3p$, 4p, $2s2p^6 3s3p4s$, $2s2p^6 3p^3$, $2s2p^6 3s3p^2$ and $2s2p^6 3s^2 3d$.

Two *bound channels* are present in the close–coupling expansion: $2s^2 2p^6 3s^2 3p$ and $2s^2 2p^6 3p^3$. The first set of configurations is present partly to describe the neutral target $2s^2 2p^6 3s^2 3p$ (*closed channel* system). The orbitals 1s, 2s, 2p, 3s, 3p, 3d, 4s and 4p are defined by their respective *scaling parameters* (Superstructure code of Eissner and Nussbaumer 1969): 1.4868, 1.1315, 1.0803, 1.1135, 1.1340, 1.1900, 1.1639 and 1.1150, respectively.

In the case of 2p–photoionization the set of configurations for the description of the ground state is the same as above, while the configurations for the states with 2p-vacancy were the following: $2s^2 2p^5 3s^2 3p$, 4p, $3p^3$, 3s3p4s, $3s3p^2$ and $3s^2 3d$. The scaling parameters for the orbitals 1s, 2s, 2p, 3s, 3p, 3d, 4s and 4p were 1.4728, 1.0617, 1.0440, 1.0064, 1.0051, 1.0493, 1.0171, 0.9985.

2.2. Shake processes probabilities

We calculate SU and SO processes in the frame of sudden perturbation theory (SPT) (Sachenko & Demekhin 1965). This approximation is valid at photon energies above the respective double excitation/ionization thresholds where SU and SO probabilities reach constant values. This saturation occurs normally at photon energies exceeding SU/SO threshold by about the binding energy of an electron being additionally excited (Kochur et al. 1990)

The probabilities of double monopole shake processes were calculated with the formula obtained by simple statistical modification of the traditional SPT formula as described by Kochur et al. (2002).

2.3. Radiationless decay rates and decay branching ratios

In order to carry out L vacancy Auger rates using the R–matrix code, we consider the reverse scattering problem $Al^{++} + e^- \rightarrow Al^+$ for large incident energies.

To obtain the probabilities of electron capture leading to formation of highly excited inner-shell vacancy states Al^+, we include in the close coupling expansion the L–vacancy *bound channel* configurations and eventually add several chosen *closed channels*.

Resonances will occur in the scattering matrix at energies in the vicinity of 2s– and 2p–vacancy states. By analyzing the resonant behaviour of the scattering matrix diagonal elements, we obtain positions and partial decay rates of those states (De Araújo & Petrini 1988). In this way the free final channel coupling is fully taken into account. This coupling is important for 2s– and 2p–vacancy states formed by free electrons with low (a few Rydbergs) energies: for the 2p–vacancy Auger–decaying into $2p^6 3s$, $2p^6 3p$, and for the 2s–vacancy decaying into $2p^5 3s3p$, $2p^5 3s^2$ via Coster–Kronig transitions.

The a priori weak channel rates will be strongly affected by dipolar coupling.

For 2p vacancy decays of $2p^5 3s^2 3p$ states, we also evaluate the shake up process associated with the Auger decay itself (Auger shake processes), for example, the probabilities for the

ejected Auger electron to excite the residual ion: $2p^5 3s^2 3p \rightarrow 2p^6 3p + e^-(E) \rightarrow 2p^6 3d + e^-(E')$

Although the processes of this kind are relatively weak, they give rise to additional line emission.

To describe the cascading decay of the states produced by photoionization one needs to know, at each decay step, the branching ratios, i.e. the probabilities for a given vacancy state to decay into each of possible final states. The decay branching ratios for various states produced during cascading decay following first–step decays were calculated in configuration-average approximation using the average partial transition widths. The latter quantities were calculated via the methods described by Kochur et al. (1994). Very briefly, the expressions for the transitions partial widths are factorized so that one term depends only on the symmetry of the atomic orbitals involved in the transition and on electron subshells occupation numbers; another term is expressed with radiation or radiationless transition integrals calculated with the wavefunctions optimized for an appropriate electron configuration.

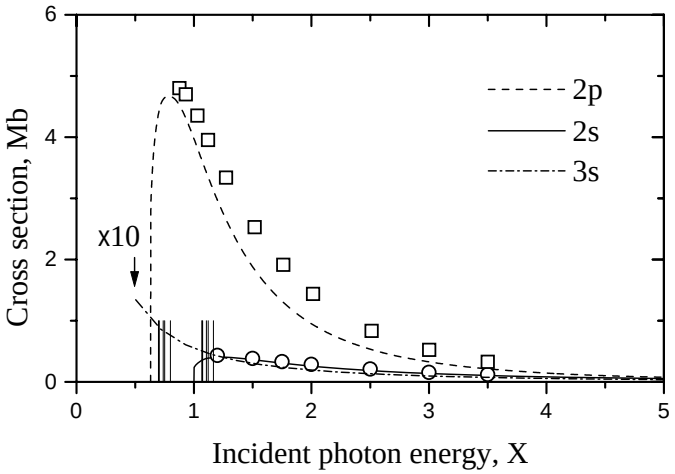

Fig. 1. Cross sections of 3s–, 2s–, and 2p–photoionization of atomic aluminium. Lines, calculation in one–configuration approximation; symbols, R–matrix technique (2s and 2p). Vertical bars show the positions of SU, cSU, and SO thresholds.

3. Results and discussion

In this section we discuss the relative importance of 2p–, 2s– and 3s–photoionization, then analyze in detail the first-step decays of the states produced by photoionization. The following decay steps are analyzed in the configuration-average approximation. Finally, we estimate relative intensities of the lines emitted at various incident photon energies.

Calculated L–shell photoionization cross sections are presented in Fig. 1.

Relative probabilities of the monopole shake up, shake off and double shake processes are listed in Table 1. It should be noted that the monopole SU processes probabilities calculated using the SPT and R–matrix approximations differ, the latter quantities being somewhat smaller. In the following discussion, we choose to use the SPT results for the SU probabilities since they are obtained without any parameterization.

The relative probabilities of 2p/cSU are shown in Fig. 2.

The partial widths of radiationless decays for relevant aluminium inner–shell hole states are presented in Tables 2 to 4.

Table 5 represents the relative intensities of emission lines produced at various incident photon energies

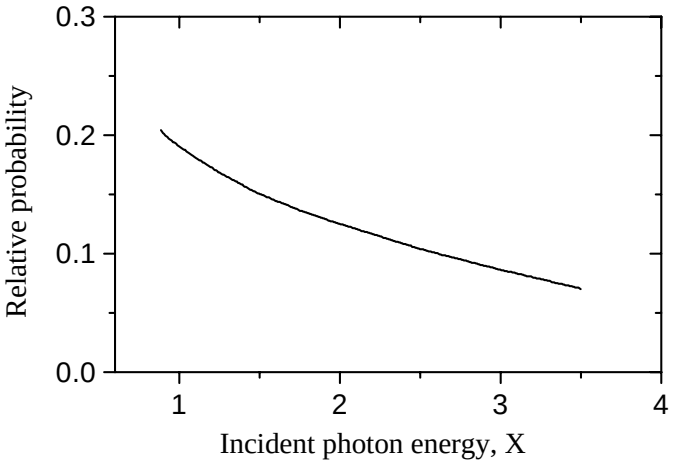

Fig. 2. Relative probability of conjugate shake up processes (3s→3p and 3p→3d) upon 2p photoionization of atomic Al.

3.1. Photoionization cross sections and shake processes probabilities

Consider the L–shell photoionization cross sections presented in Fig. 1. Lines and symbols in Fig. 1 represent the cross sections, vertical bars show the positions of the thresholds for SU, cSU and SO processes upon 2s– and 2p– ionization.

Configuration–average one–electron results are represented with lines, while the R-matrix results are shown with symbols. Note that the results obtained in those two approximations compare well.

The cross section of 2p–photoionization (dash line and squares) dominates the 2s one (solid line and circles) over a wide energy range. It is about ten times greater than 2s at the 2s threshold, however, descending more rapidly than the 2s cross section, it is about twice the 2s at $X = 3.2$ (≈400 eV) and becomes equal to 2s at $X = 7$ (≈900 eV).

Also shown in Fig. 1 is the cross section of 3s-photoionization calculated using the one-electron approximation (dash–dot line). Single 3s–photoionization is responsible for the production of the Al II emission. One can see that 3s–photoionization is not negligible in the energy range of interest.

Relative probabilities of the monopole shake processes (SU, SO and dS) upon 2s and 2p sudden vacancy creation are presented in Table 1. One can see that the effect of the initial inner–shell vacancy is small, which is what one would have expected (Kochur et al. 2002). The SU processes dominate both for the shakes from 3s and from 3p subshells having relative probability of about 8% and 13%, respectively. The probabilities of the SO processes are smaller, 1.6 to 2%.

For monopole double shake processes the approximation used does not allow one to distinguish accurately between up and off processes, therefore the values presented

Table 1. Relative probabilities of monopole shake processes upon L-shell ionization of atomic Al.

Initial vacancy	Process	Relative probability*
2s	2s/SU 3s → 4s	0.0752
	2s/SU 3s → 5s	0.0067
	2s/SO 3s → εs	0.0190
	2s/SU 3p → 4p	0.1216
	2s/SU 3p → 5p	0.0088
	2s/SO 3p → εp	0.0164
	2s/dS 3s3s→ $\{n', \varepsilon'\}$s,$\{n'', \varepsilon''\}$s	0.0021
	2s/dS 3s3p→ $\{n', \varepsilon'\}$s,$\{n'', \varepsilon''\}$p	0.0116
2p	2p/SU 3s → 4s	0.0817
	2p/SU 3s → 5s	0.0073
	2p/SO 3s → εs	0.0161
	2p/SU 3p → 4p	0.1194
	2p/SU 3p → 5p	0.0086
	2p/SO 3p → εp	0.0162
	2p/dS 3s3s→ $\{n', \varepsilon'\}$s,$\{n'', \varepsilon''\}$s	0.0025
	2p/dS 3s3p→ $\{n', \varepsilon'\}$s,$\{n'', \varepsilon''\}$p	0.0126

* With respect to the probability of single 2s/2p ionization.

in Table 1 combine all possible contributions, i.e. SU+SU, SU+SO, SO+SO. However, rough estimates show that the relative importance of those contributions are the following: (SU+SU):(SU+SO):(SO+SO) ≈ 0.6:0.2:0.2.

The R–matrix relative probability of conjugate shake up processes upon 2p photoionization is shown in Fig. 2 as a function of incident photon energy. The 3p→3d excitation dominates. The whole cSU effect is extremely dependent on the 3d excited orbital definition since the CI between the $n = 3$ states is significant. In contrast to the monopole shake processes whose probability comparatively rapidly (for outermost shells) reach a constant limit, the relative probability of the cSU processes decreases with energy. However, it is evident from Fig. 2 that over quite a wide energy range the cSU excitations are important.

Since both monopole and conjugate shake probabilities in Table 1 and Fig. 2 are relative to their respective main processes, one can easily obtain the cross sections for the shake processes by multiplying the relative probabilities by the respective main processes cross sections. For example, the cross section for the 2p/SU 3s→4s process at $X = 1.5$ is
P(2p/SU 3s→4s)×σ_{2p}(1.5) = 0.817×1.9 = 1.55 Mb.

3.2. Line emission upon decay of the states produced by photoionization

3.2.1. Line emission after 3s photoionization

It is evident from Fig. 1 that within the energy range of interest, 3s–photoionization is not negligible, making up about 2% of L–ionization. Photoionization of the 3s–subshell directly produces the line emitting states Al II $3s3p^{1,3}P$. This is the only mechanism of the Al II emission in this incident photon energy range.

3.2.2. Line emission after 2p–photoionization

Single 2p–ionization produces a single inner-shell hole Al $2p^{-1}$ state which in the one-configuration approximation can decay non-radiatively via two Auger transitions, i.e. $L_{23}M_1M_1$ and $L_{23}M_1M_{23}$ giving rise to the states $2p^63p\ ^2P$ and $2p^63s\ ^2S$. The processes of additional excitations during the Auger transitions may lead to formation of additional decay channels leading to the states $2p^63d$, $2p^64s$, $2p^64p$ (see Table 2). The ionic $2p^63s$ ground state can decay no further, while all other states are line-emitting.

Our calculation showed that the population of final states during 2p–photoionization is proportional to their statistical weights. Then using the partial widths Γ_{LS}(i − f) of Table 2 it is easy to calculate the branching ratios for the decays from initial state $i = 2p^53s^23p$ into each of the final states f = 3s, 3p, 3d, 4s, 4p:

$$\chi(i-f) = \sum_{LS} \frac{g_{LS}}{g_i} \frac{\Gamma_{LS}(i-f)}{\sum\limits_f \Gamma_{LS}(i-f)}$$

where LS are the initial state terms, g_{LS} are their statistical weights, and g_i is the statistical weight of the initial configuration.

The decay process for single 2p–vacancy state can be illustrated with the following decay scheme:

$$\begin{aligned} &2p^53s^23p \qquad (1)\\ &\quad\longrightarrow(0.335)2p^63s\\ &\quad\longrightarrow(0.607)2p^63p \rightarrow\rightarrow 2p^63s\\ &\quad\longrightarrow(0.033)2p^63d \rightarrow\rightarrow 2p^63p \rightarrow\rightarrow 2p^63s\\ &\quad\longrightarrow(0.009)2p^64s \rightarrow\rightarrow 2p^63p \rightarrow\rightarrow 2p^63s\\ &\quad\longrightarrow(0.016)2p^64p\\ &\qquad\qquad\rightarrow\rightarrow(0.420)2p^63s\\ &\qquad\qquad\rightarrow\rightarrow(0.580)2p^63d \rightarrow\rightarrow 2p^63p \rightarrow\rightarrow 2p^63s. \end{aligned}$$

Table 2. Auger widths for the decay of the Al $2p^5 3s^2 3p$ states in units of 10^{-4} a.u. E is the initial state energy in Ryd.

Initial states		Final states[1]				
Term	E^2	3s	3p	3d	4s	4p
^{3}S	4.291	0.84	0.043	0.003	0.006	0.001
^{3}D	4.304	0.0505	0.0609	0.0049	0.0019	0.0015
^{1}D	4.384	0.134	0.194	0.0075	0.0042	0.0018
^{1}P	4.388	0.0	0.0326	0.0004	0.0	0.0003
^{3}P	4.390	0.0	0.264	0.013	0.0	0.011
^{1}S	4.706	51.08	2.65	0.27	0.36	0.12

[1] In notations of configurations filled subshells are omitted.
[2] With respect to the 3s ground state.

Here the branching ratios (given in parentheses) are calculated for the first decay step using the data of Table 2, and for the following decays, in a configuration-average one-electron approximation. Radiationless transitions are shown with arrows while radiative transitions are shown with double arrows. These denotations will be preserved in the following discussion.

One can see from the scheme (1) that the decay of the states produced by single 2p–photoionization gives rise to five Al III lines of which the strongest is Al III 3p-3s. In about 60% of cases when 2p photoionization happens this line will be emitted.

The SO processes upon 2p–photoionization do not lead to line emission. Indeed, if either a 3s or 3p electron is shaken off, then the consequent $L_{23}MM$ Auger transition will end up in the ground state of Al IV.

The channel for the 2p/SU 3s→4s process is opened at 1.01 Ryd above the 2p threshold. Its relative probability reaches its SPT limit of 0.0817 at about twice this energy above the SU threshold, i.e. at about $X = 0.85$. The shake–up state thus produced decays via the following scheme:

$$
\begin{aligned}
&2p^5 3s3p4s \qquad (2)\\
&\quad \longrightarrow (0.869)2p^6 4s \rightarrow\rightarrow 2p^6 3p \rightarrow\rightarrow 2p^6 3s\\
&\quad \longrightarrow (0.002)2p^6 3p \rightarrow\rightarrow 2p^6 3s\\
&\quad \longrightarrow (0.129)2p^6 3s.
\end{aligned}
$$

The channel for the 2p/SU 3p→4p is opened at 0.695 Ryd above the 2p–threshold, the probability of the process reaching its SPT limit of 0.119 at about $X = 0.78$. The state produced by the 2p/SU 3p→4p process decays via the following scheme:

$$
\begin{aligned}
&2p^5 3s^2 4p \qquad (3)\\
&\quad \longrightarrow (0.968)\ 2p^6 3s\\
&\quad \longrightarrow (0.032)\ 2p^6 4p\\
&\qquad\qquad \rightarrow\rightarrow (0.420)2p^6 3s\\
&\qquad\qquad \rightarrow\rightarrow (0.580)2p^6 3d \rightarrow\rightarrow 2p^6 3p \rightarrow\rightarrow 2p^6 3s.
\end{aligned}
$$

One can see from Fig. 2 that the conjugate shake–up process occurs with significant probability upon 2p–photoionization. The decays of the states thus produced are shown in the following schemes.

After 2p/cSU 3p→3d:

$$
\begin{aligned}
&2p^5 3s^2 3d \qquad (4)\\
&\quad \longrightarrow (0.980)2p^6 3s\\
&\quad \longrightarrow (0.020)2p^6 3d \rightarrow\rightarrow 2p^6 3p \rightarrow\rightarrow 2p^6 3s.
\end{aligned}
$$

After 2p/cSU 3s→3p:

$$
\begin{aligned}
&2p^5 3s3p^2 \qquad (5)\\
&\quad \longrightarrow (0.513)2p^6 3s\\
&\quad \longrightarrow (0.487)2p^6 3p \rightarrow\rightarrow 2p^6 3s.
\end{aligned}
$$

As discussed above, monopole double shake processes upon 2p–photoionization are rather weak, 1.5% in total upon 2p ionization, 2p/dS 3s3p dominating (1.3%). Analysis of the decay processes showed that the states produced by SU+SU dS do not give any lines different from those produced by single photoionization process, and the states produced by the SU+SO decay non-radiatively into ionic ground states giving no emission. The SO+SO dS, however weak, produce an Al IV $2p^5 3s \rightarrow 2p^6$ doublet. The thresholds for the 2p/dS processes lie at about $X = 1$.

3.2.3. Line emission after 2s–photoionization

Table 3 lists the widths of radiationless decays of the single 2s–vacancy state produced by photoionization. Single 2s vacancy in aluminium decays through two Coster–Kronig ($L_1L_{23}M_1$, $L_1L_{23}M_{23}$) and two Auger ($L_1M_1M_1$, $L_1M_1M_{23}$) transitions. Among the states produced at the first decay step only the state $2p^6 3p$ reached by the $L_1M_1M_1$ Auger transition is obviously line emitting (Al III 3p-3s). The state $2p^5 3s^2$ decays further non–radiatively into $2p^6$ and gives no emission, and $2p^6 3s$ is the ionic ground state.

The state $2p^5 3s3p$ is produced by the Coster-Kronig $L_1L_{23}M_1$ transition; its quadruplet terms and both ^{2}P terms have a zero radiationless decay width in the LS–coupling approximation. One might then expect to have emission from those states. However, the presence of the 2p–vacancy leads to noticeable spin-orbital interaction, which makes radiationless decays of those states possible. Our intermediate–coupling calculation using Badnell's code (Badnell 1985) showed that respective decays dominate radiative ones.

Table 3. Non-radiative widths for the decay of the Al $2s2p^63s^23p$ state in units of 10^{-4} a.u.

Transition	Final state			Initial state[1] $^1P^o$	Initial state[1] $^3P^o$
$L_1L_{23}M_1$	$2p^53s3p$	^2S	upper	1.0	15.8
		^2P		18.0	40.9
		^2D		17.0	37.3
		^2S	lower	51.2	12.6
		^2P		73.6	51.8
		^2D		118.3	95.8
		^4P		0.0	2.7
		^4D		0.0	6.6
		^4S		0.0	1.3
$L_1L_{23}M_{23}$	$2p^53s^2$	$^2P^o$		33.3	41.5
$L_1M_1M_1$	$2p^63p$	$^2P^o$		2.4	1.3
$L_1M_1M_{23}$	$2p^63s$	^2S		0.6	4.2
Level width in a.u.				0.0315	0.0312

[1] Initial $^1P^o$ and $^3P^o$ states energies are 7.821 Ryd and 7.774 Ryd, respectively.

Table 4. Auger widths for the decay of the states produced by 2s/SO processes (in units of 10^{-4} a.u.). E are initial states energies in Rydbergs.

Initial state		E[1]	Final states: $2p^6$	$2p^53s$ $^3P^o$	$2p^53s$ $^1P^o$	$2p^53p$ ^3S	$2p^53p$ ^3D	$2p^53p$ ^1D	$2p^53p$ ^3P	$2p^53p$ ^1P	$2p^53p$ ^1S
$2s2p^63s^2$	^2S	6.57	3.0	32.0	226.0	0.6	3.6	0.2	0.0	0.0	0.1
$2s2p^63s3p$	$^4P^o$	6.96	0.0	47.2	0.0	19.3	109.5	0.0	80.6	0.0	0.0
	$^2P^o$	7.07	1.9	21.0	21.0	9.78	47.1	14.2	29.4	11.3	2.6
	$^2P^o$	7.36	5.16	11.0	8.4	0.82	4.78	88.0	2.02	46.1	24.2

[1] With respect to $2p^5$ Al IV ground state.

Having found that the singlet and triplet terms are populated proportionally to their statistical weights and using the widths listed in Table 3 we find that the decay process for the single 2s hole state can be summarized in the following way:

$$
\begin{aligned}
&2s2p^63s^23p \qquad (6)\\
&\longrightarrow (0.859)2p^53s3p \longrightarrow 2p^6\\
&\longrightarrow (0.125)2p^53s^2 \longrightarrow 2p^6\\
&\longrightarrow (0.010)2p^63s\\
&\longrightarrow (0.005)2p^63p \rightarrow\rightarrow 2p^63s.
\end{aligned}
$$

One can see that single 2s–photoionization produces a single Al III line with a rather weak probability of 0.005.

The states produced by 2s/SU, 2s/cSU, and 2s/dS decay via consecutive radiationless transition into $2p^6$ giving no emission.

The partial widths for the decay of the states produced by the 2s/SO processes, i.e. $2s2p^63s^2$ and $2s2p^63s3p$, are listed in Table 4. Note that from $2s2p^63s^2$, reaching $2p^53p$ is possible due to CI, and those transitions correspond to additional excitations during Coster–Kronig decay.

The decay of the 2s/SO states give rise to a set of states emitting Al IV lines according to the following decay schemes:

After 2s/SO 3p$\rightarrow \varepsilon$p:

$$
\begin{aligned}
&2s2p^63s^2 \qquad (7)\\
&\longrightarrow (0.971)\ 2p^53s \rightarrow\rightarrow 2p^6\\
&\longrightarrow (0.012)\ 2p^6\\
&\longrightarrow (0.017)\ 2p^53p \rightarrow\rightarrow 2p^53s \rightarrow\rightarrow 2p^6.
\end{aligned}
$$

After 2s/SO 3s$\rightarrow \varepsilon$s:

$$
\begin{aligned}
&2s2p^63s3p \qquad (8)\\
&\longrightarrow (0.807)\ 2p^53p \rightarrow\rightarrow 2p^53s \rightarrow\rightarrow 2p^6\\
&\longrightarrow (0.178)\ 2p^53s \rightarrow\rightarrow 2p^6\\
&\longrightarrow (0.015)\ 2p^6.
\end{aligned}
$$

One can see from (7, 8) that the 2s/SO processes lead to emission of additional lines, i.e. Al IV $2p^53p\ ^{1,3}SDP–2p^63s\ ^{1,3}P$. Of these, the most intense ones should be the lines originating from ^3D and ^1D terms (see Table 4)

3.3. Relative intensities of emitted lines

To be able to compare the probabilities of emission for various lines, let us define the partial cross section for

Table 5. Line emission cross sections (in Mb).

Transition	Incident photon energy in units of X						
	0.60	0.66	0.98	1.04	1.40	2.00	4.00
Al II $3s3p–3s^2$	0.112	0.099	0.058	0.052	0.034	0.019	0.006
Al III 3p–3s		2.504	3.195	2.909	1.642	0.773	0.100
Al III 3d–3p		0.161	0.190	0.173	0.098	0.043	0.007
Al III 4s–3p		0.034	0.329	0.300	0.176	0.152	0.012
Al III 4p–3s		0.254	0.280	0.255	0.150	0.065	0.010
Al III 4p–3d		0.035	0.047	0.043	0.025	0.011	0.002
Al IV $2p^5 3s–2p^6$					0.046	0.023	0.005
Al IV $2p^5 3p–2p^5 3s$					0.006	0.004	0.001
L–photoionization cross section		3.804	4.093	4.048	2.572	1.203	0.226

L–photoionization ending in the emission of a specific line in the following manner:

$$\sigma(C_\mathrm{i} - C_\mathrm{f}) = \sum_{l=\mathrm{s,p}} \sigma_{2l} \sum_{\alpha} P_{2l}\,(\alpha; C_\mathrm{i} - C_\mathrm{f})\,. \qquad (9)$$

Here C_i and C_f are the initial and final configuration of a line–emitting transition, σ_{2l} is either the 2s– or 2p–photoionization cross section, $P_{2l}\,(\alpha; C_\mathrm{i} - C_\mathrm{f})$ is the relative (to respective single ionization process) probability of emitting the $C_\mathrm{i} - C_\mathrm{f}$ line via the process α, α is one of the processes leading to line emission, i.e. single 2p/2s–ionization, 2p/SU 3s→4s, etc.

The values $\sigma(C_\mathrm{i} - C_\mathrm{f})$ when multiplied by spectral photon flux at certain photon energies give line emission rates per unit incident photon energy interval. On the other hand, the values $\sigma(C_\mathrm{i} - C_\mathrm{f})/(\sigma_{2\mathrm{p}}+\sigma_{2\mathrm{s}})$ are the probabilities of line emission upon the condition that L–photoionization took place at certain energy.

For the Al II $3s3p–3s^2$ doublet, it is clear that its partial cross section coincides with the 3s–photoionization cross section.

We calculated the partial emission cross sections (9) for emission lines discovered for the following incident photon energies (in units of X): 0.60 (below 2p–threshold), 0.66 (right above the 2p–threshold, all shake channels are closed), 0.98 (2p/shake channels are opened, 2s–ionization is closed), 1.04 (right above the 2s–threshold, 2s/shake and 2p/dS channels are closed), 1.40 (2s/shake and 2p/dS channels are opened), 2.00, 4.00.

Calculated partial emission cross sections are listed in Table 5. The bottom line of Table 5 lists the total Al L–photoionization cross section.

4. Conclusions

Photoionization of atomic aluminium in the region from 80 to several hundred eV leads to emission of a number of Al II, Al III and Al IV lines. Relative intensities of all the emission lines change as the incident photon energy increases due to opening of channels for various processes, like single photoionization, shake up or shake off processes.

Monopole and conjugate shake up, shake off and double shake off processes upon photoionization, as well as similar processes upon Auger and Coster–Kronig decay of the states produced by photoionization, play an important role in line emission.

Low–intensity Al II $3s3p–3s^2$ is emitted due to 3s–photoionization which is not negligible in the energy range of interest.

2p–photoionization is the principal producer of Al III line emission. The most intense line emitted upon single 2p–photoionization is Al III 3p–3s 1857 Å UV line. A number of other Al III lines are emitted due to double processes upon 2p–photoionization. Their intensities are roughly one order of magnitude less.

The single 2s–photoionization gives rather little emission since the 2s–vacancy decays non-radiatively into ionic ground states. On the other hand, the shake off processes upon 2s–photoionization contribute to Al IV emission.

Acknowledgements. AGK would like to thank his colleagues from Laboratoire Cassini UMR 6529 for their hospitality during his stay in Nice. This work was partly supported by the fundamental research grant from Russian Ministry of Railway Transport (No 510(9)/2001)

References

Amusia, M. Ya., & Cherepkov, N. A. 1975, Case Studies in Atomic Physics 2, No 2, 47
Badnell, N. R. 1985, Cambridge Department of Applied Mathematics and Theoretical Physics Report DAMTP/AA/–1001–NRB
Badnell, N. R., Petrini, D., & Stoika, S. J. 1997, Phys. B. At. Mol. Opt. Phys., 30, L665
Berrington, K. A., Eissner, W. B., & Norrington, W. B. 1995, Comput. Phys. Commun., 92, 290
Carlson, T. A., & Nestor, C. W. Jr 1973, Phys. Rev. A, 8, 2887
De Araújo, F. X., & Petrini, D. 1988, J. Phys. B, 21, L117
Eissner, W., & Nussbaumer, H. 1969, J. Phys. B, 2, 1028
Indelicato, P., Boucard, S., & Lindroth, E. 1998, Eur. Phys. J., 3, 29
Kau, R., Petrov, I. D., Sukhorukov, V. L., & Hotop, H. 1997, Z. Phys. D., 39, 267
Kochur, A. G., Nadolinski, A. M., & Sukhorukov, V. L. 1990, Optika i Spektroskopiya (USSR), 69, 464
Kochur, A. G., Dudenko, A. I., Sukhorukov, V. L., & Petrov, I. D. 1994, J. Phys. B. At. Mol. Opt. Phys., 27, 1709
Kochur, A. G., Petrini, D., & da Silva, E. P. 2001, A&A, 365, 248
Kochur, A. G., Dudenko, A. I., & Petrini, D. 2002, J. Phys. B. At. Mol. Opt. Phys., 35, 395
Sachenko, V. P., & Demekhin, V. F. 1965, J. Exper. Theor. Phys. (USSR), 49, 765
Sukhorukov, V. L., Demekhin, V. F., Timoshevskaya, V. V., & Lavrentiev, S. V. 1979, Optika i Spektroskopiya (USSR), 47, 407
Weisheit, J. C. 1974, ApJ, 190, 735